Automotive Science and Engineering, Vol. 11, No. 3, (2021), 3579-3593

Iran University of Science and Technology

Automotive Science and Engineering

Journal Homepage: ase.iust.ac.ir

ISSN: 2008-9899

A PDE-based approach to internal and string stability analysis of large-scale bi-directional vehicular convoys

Hossein Chehardoli*

Department of Mechanical Engineering, Ayatollah Boroujerdi University, Boroujerd, Iran.

ARTICLE INFO

Article history:
Received: 12 April 2021
Accepted: 10 Aug 2021
Published: 1 Sep 2021

Keywords:
Large-scale vehicular convoys
Internal stability
String stability
PDE-based approach
Decoupling

A B S T R A C T

This paper considers the asymptotic zero tracking error as well as string stability of large-scale automated vehicle convoys (LAVC). Both centralized and decentralized bi-directional network topologies are investigated. A double integrator dynamical equation is defined to describe the 1-D dynamics of automated vehicles (AV). A centralized / decentralized controller which employs the relative displacement and velocity compared with the backward and forward AVs is defined for all following AVs. Since the dynamical equation of LAVC is hard to be analyzed for internal stability, a PDE-based approach is introduced to decouple and reduce the closed-loop dynamical equation. According to this approach, we will be able to decouple the dynamical equation of all AVs individually based on the error dynamics. After simplifying the dynamical equation of LAVC, the conditions satisfying the internal stability of centralized and decentralized networks are obtained. After that, algebraic analyses in frequency domain will able us to find the constraints on control gains guaranteeing the string stability. Simulation and experimental results are available to describe the merits of this algorithm.

1. Introduction

The problem of traffic congestion has been a significant social, economical and environmental issue in all societies. Numerous undesirable outcomes such as noise/air pollution, time/fuel wasting, decreasing road capacity and safety, etc., are the results of traffic jams [1, 2]. The coordinated movement of AVs with the same constant speed and safe distances between AVs is called vehicle convoying (VC). The VC is an applicable and efficient method to implement the intelligent transportation systems (ITS) [3].

The controller configuration of an AV is composed of two hierarchical levels. 1) High-level controller by employing several information such as the position of AV in the convoy, desired velocity, desired inter-AV distance, etc., computes the appropriate acceleration of the AV to follow the desired velocity specified by leading AV [4]. 2) Low-level controller receives the acceleration information sent by the high-level controller and sends the necessary rules to the braking and throttling systems to maintain the AV in the appropriate position in the convoy [5].

Three approaches are used to tune the inter-AV distances in a LAVC. 1) Constant Distance approach (CDA): the distance between subsequent AVs is always fixed. So that, the convoy's length is always constant [6]. 2) Constant time headway approach (CTHA): the elapsed time by an AV to reach the forward vehicle's position is always fixed. Therefore, the inter-vehicle distances and the convoy's length will vary by changing the leader velocity [7] and 3) mixed distance approach

*Corresponding Author
Email Address: h.chehardoli@abru.ac.ir
https://doi.org/10.22068/ase.2021.587

(MDA): the inter-AV distance is a function of the convoy's velocity [8]. In a centralized network, the leading AV is connected with all following AVs. While in a decentralized convoy, some followers are not able to communicate with the leading AV [9].

Two types of stability are considered in a convoy. 1) Asymptotic stability (internal stability): in which the distance tracking errors between all following AVs and the leading AV tend to zero asymptotically, the convoy is called internal (asymptotic) stable [3] and 2) string stability: in which the maximum value of distance errors has a decreasing trend along with the convoy [10]. There is a direct relation between the inter-AV distance approach and the string stability. For example, in decentralized networks with CDA, the string stability will not be satisfied [6].

The large number of research works on VC can be categorized from different aspects. 1) Linear control approaches: safety/comfort analysis [11], MPC [12, 13], scalability [14], etc. 2) Nonlinear methods: Robust control [15], adaptive control [7], etc. 3) Time delay analysis [16]. 4) Centralized [6], decentralized [9], MLA [17], unidirectional [7], bi-directional [18] and complex [6] network topology. 5) String stability under different constraints [19]. 6) Homogeneous [20, 21] and non-homogenous vehicular convoys [5] and 7) inter-AV distancing: CDA [22], CTHA [10] and MDA [8].

In a LAVC, each AV communicates with its neighbors. So that, the closed-loop dynamics has a large dimension and therefore, the stability analysis may be difficult or even impossible. A large number of previous approaches can be applied only on convoys with a finite number of following AVs [4, 6, 8, 14, 20]. A decentralized unidirectional protocol is designed in [4] to assure stability in the presence of time delay. The results are verified by experimental studies. The non-uniform network topology is studied in [6]. In this paper, only the internal stability is studied, and the authors could not solve the string stability. The calculating of the stability margin in the presence of time delay in the frequency domain is presented in [14]. In [20], a second-order consensus law is designed to achieve the internal as well as string stability of centralized unidirectional networks. A leader following control method is introduced in [23] to achieve the third-order global consensus of homogeneous VCs. In [24], a centralized controller is designed to guarantee the stability under switching topology. Internal stability under the complex topologies is investigated in the following works [6, 8, 25]. None of these methods and similar works cannot be generalized on LAVCs. Moreover, if the communication topology switches between different configurations, the stability analysis will be more complicated [24]. On the other hand, the string stability of LAVCs is also challenging as well as the internal stability. Most of the previous methods, are not able to achieve to internal and string stability of LAVCs. Therefore, presenting a general solution for both of internal and string stability of centralized and decentralized bi-directional large-scale vehicle networks is necessary.

Motivated by the mentioned defects, to obtain a comprehensive approach for internal and string stability of LAVCs, we present a novel method to decouple the dynamical equation of large-scale centralized/decentralized bi-directional VCs. A double integrator model is introduced to describe the 1-D dynamics of each following AV. A linear consensus scheme is proposed for following AVs utilizing the relative information (displacement and velocity) between forward and backward AVs. A PDE-based approach is developed to simplify the dynamical equation of each following AV and consequently, the essential constraints on control parameters satisfying stability (internal and string) will be obtained. The effectiveness of the proposed approach is illustrated by verification studies (numerical and experimental). The most important novelties of this paper are: presenting a new PDE-based approach assuring internal and string stability for bi-directional LAVCs.

The remainder of our work is constructed as follows. Section 2 studies the internal stability of both centralized and decentralized networks. Section 3 solves the string stability problem. In section 4, the related numerical and experimental results are presented to depict the advantages of our method. In the end of this paper, the conclusion is presented.

2. Internal stability analysis

Fig. 1 depicts an AV convoy in longitudinal motion. This convoy consists of a leader and following AVs.

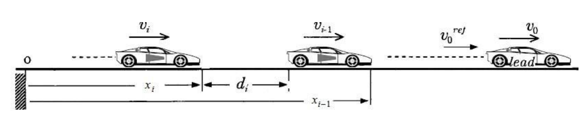

Figure 1: An AV convoy in longitudinal motion.

2.1. Longitudinal AV dynamics

The following double integrator model describes the high-level dynamical equation of an AV [15, 43, 51, 54]:

$$m_i\ddot{x}_i = \overline{u}_i \Rightarrow \ddot{x}_i = \overline{u}_i / m_i = u_i \quad (1)$$

where $\ddot{x}_i = a_i, m_i$ and u_i denote the acceleration, mass and control law of the i-th AV, respectively. The controller is designed for two main network configurations centralized and decentralized communication topology.

2.2. Centralized control design

For centralized network, the following control protocol is introduced for the i-th AV $(i = 1,2,...,N-1)$

$$\begin{aligned} u_i &= -\alpha_i^f (x_i - x_{i-1} + D_{i-1,i} + L_{i-1}) - \gamma_i^f (\dot{x}_i - \dot{x}_{i-1}) \\ &\quad -\alpha_i^b (x_i - x_{i+1} - D_{i,i+1} - L_i) - \gamma_i^b (\dot{x}_i - \dot{x}_{i+1}) \\ &\quad -\eta_i (\dot{x}_i - \dot{x}_0) \end{aligned} \quad (2)$$

where α_i^f and α_i^b are the forward and backward displacement gains, γ_i^f and γ_i^b are the forward and backward velocity gains, respectively and η_i is the relative velocity gain with respect to the leader. Moreover, L denotes the AV's length and D is the minimum inter-AV distance. For the last AV, the control law is designed as follows.

$$\begin{aligned} u_N &= -\alpha_N^f (x_N - x_{N-1} + D_{N-1,N} + L_{N-1}) \\ &\quad -\gamma_N^f (\dot{x}_N - \dot{x}_{N-1}) - \eta_N (\dot{x}_N - \dot{x}_0) \end{aligned} \quad (3)$$

The following figure depicts the dynamics of the closed-loop of i-th AV in the convoy.

Combining (1) and (2) will result to

$$\begin{aligned} a_i &= -\eta_i (\dot{x}_i - \dot{x}_0) - \gamma_i^f (\dot{x}_i - \dot{x}_{i-1}) \\ &\quad -\alpha_i^f (x_i - x_{i-1} + D_{i-1,i} + L_{i-1}) \\ &\quad -\alpha_i^b (x_i - x_{i+1} - D_{i,i+1} - L_i) \\ &\quad -\gamma_i^b (\dot{x}_i - \dot{x}_{i+1}) \end{aligned} \quad (4)$$

Based on CDA, the desired position of the i-th AV is considered as

$$x_{i,d}(t) = x_0 - D_{0,i} - \sum_{j=1}^{i-1} L_j = x_0 - \sum_{j=1}^{i} (D_{j-1,j} + L_{j-1}) \quad (5)$$

where $D_{0,i}$ is the desired distance between the leader and the i-th AV. We define the displacement tracking error according to

$$e_i = x_i - x_{i,d} \Rightarrow \quad \dot{e}_i = \dot{x}_i - \dot{x}_{i,d} \Rightarrow \quad \ddot{e}_i = \ddot{x}_i \quad (6)$$

By rewriting (4) in terms of tracking error and knowing that $x_{i-1,d} - x_{i,d} = D_{i-1,i} - L_{i-1}$, one can write

$$\begin{aligned} \ddot{e}_i &= -\alpha_i^f (e_i - e_{i-1}) - \gamma_i^f (\dot{e}_i - \dot{e}_{i-1}) \\ &\quad -\alpha_i^b (e_i - e_{i+1}) - \gamma_i^b (\dot{e}_i - \dot{e}_{i+1}) - \eta_i \dot{e}_i \end{aligned} \quad (7)$$

By defining that $\mathbf{E} = [e_1, \dot{e}_1, e_2, \dot{e}_2, \ldots, e_N, \dot{e}_N]^T$, the dynamics of the closed-loop of the convoy will be as follows

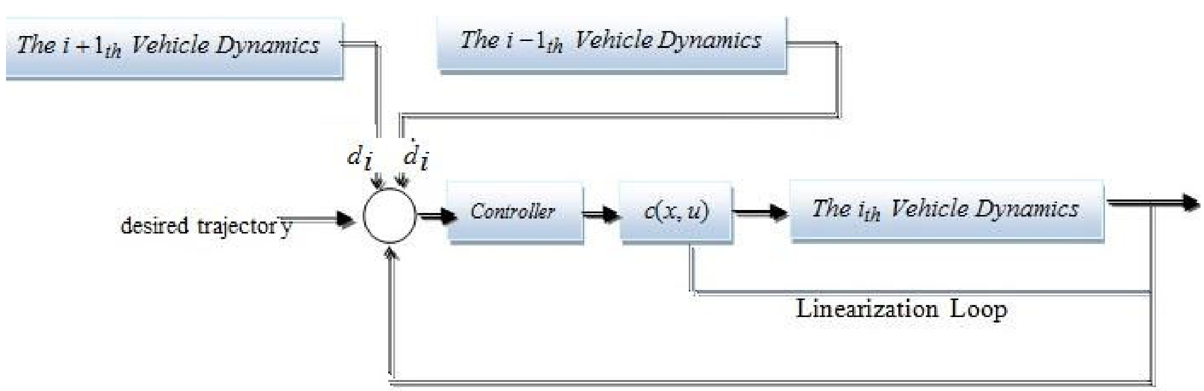

Figure 2: The dynamics of the closed-loop of i-th AV in the convoy.

$$\dot{\mathbf{E}} = \mathbf{A}\mathbf{E} \tag{8}$$

where

$$\mathbf{A} = \begin{bmatrix} \mathbf{A}_1 & \mathbf{A}_{1b} & \mathbf{0}_{2\times2} & \mathbf{0}_{2\times2} & \dots & \mathbf{0}_{2\times2} & \mathbf{0}_{2\times2} \\ \mathbf{A}_{2f} & \mathbf{A}_2 & \mathbf{A}_{2b} & \mathbf{0}_{2\times2} & \dots & \mathbf{0}_{2\times2} & \mathbf{0}_{2\times2} \\ \mathbf{0}_{2\times2} & \mathbf{A}_{3f} & \mathbf{A}_3 & \mathbf{A}_{3b} & \dots & \mathbf{0}_{2\times2} & \mathbf{0}_{2\times2} \\ \vdots & \vdots & \vdots & \vdots & \vdots & \vdots & \vdots \\ \mathbf{0}_{2\times2} & \mathbf{0}_{2\times2} & \mathbf{0}_{2\times2} & \mathbf{0}_{2\times2} & \dots & \mathbf{A}_{Nf} & \mathbf{A}_N \end{bmatrix},$$

$$\mathbf{A}_i = \begin{bmatrix} 0 & 1 \\ -\left(\alpha_i^f + \alpha_i^b\right) & -\left(\gamma_i^f + \gamma_i^b\right) \end{bmatrix}, \ \mathbf{A}_{if} = \begin{bmatrix} 0 & 0 \\ \alpha_i^f & \gamma_i^f \end{bmatrix}$$

and $\mathbf{A}_{ib} = \begin{bmatrix} 0 & 0 \\ \alpha_i^b & \gamma_i^b \end{bmatrix}$.

Calculating the eigenvalues of matrix $\mathbf{A}$ for large-scale networks is complicated or even impossible. In this paper, by employing a PDE model, we will decouple the $2N \times 2N$ order dynamical model (8) to a double integrator dynamical model. Therefore, the complications of internal stability will dramatically reduce.

For simplicity, the following definitions are introduced.

$$\begin{aligned} \alpha_i^{f+b} &= \alpha_i^f + \alpha_i^b \\ \alpha_i^{f-b} &= \alpha_i^f - \alpha_i^b \\ \gamma_i^{f+b} &= \gamma_i^f + \gamma_i^b \\ \gamma_i^{f-b} &= \gamma_i^f - \gamma_i^b \end{aligned} \tag{9}$$

Therefore, (7) can be written as follows:

$$\begin{aligned} \ddot{e}_i + \eta_i \dot{e}_i = &-\frac{\alpha_i^{f+b} + \alpha_i^{f-b}}{2}(e_i - e_{i-1}) \\ &-\frac{\alpha_i^{f+b} - \alpha_i^{f-b}}{2}(e_i - e_{i+1}) \\ &-\frac{\gamma_i^{f+b} + \gamma_i^{f-b}}{2}(\dot{e}_i - \dot{e}_{i-1}) \\ &-\frac{\gamma_i^{f+b} - \gamma_i^{f-b}}{2}(\dot{e}_i - \dot{e}_{i+1}) \end{aligned} \tag{10}$$

For simplifying the internal stability analysis, we transform the 1-*D* coordinate of longitudinal convoy dynamics to a new coordinate in the interval [0,1]. In the new coordinate, the *i*-th AV position is at $(N-i)/N$ as shown in Fig. 3.

To derive the PDE approximation, we define the new function $e_i(p,t):[0,1]\times[0,\infty) \to R.$ Where *p* is a new variable in the new coordinate. This function satisfies $e_i(t) = e(p,t)|_{p=(N-i)/N}$. According to the new coordinate, we define the following functions.

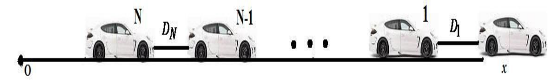

a) original coordinate

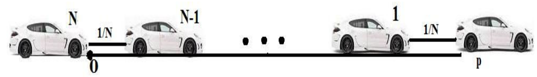

b) new coordinate

Figure 3: Original and new convoy coordinates.

$$\begin{aligned} \alpha_i^f &= \alpha^f(p)|_{p=(N-i)/N}, \\ \alpha_i^b &= \alpha^b(p)|_{p=(N-i)/N}, \\ \gamma_i^f &= \gamma^f(p)|_{p=(N-i)/N}, \\ \gamma_i^b &= \gamma^b(p)|_{p=(N-i)/N} \end{aligned} \tag{11}$$

We can write

$$\begin{aligned} &-\frac{\alpha_i^{f+b} + \alpha_i^{f-b}}{2}(e_i - e_{i-1}) \\ &\quad -\frac{\alpha_i^{f+b} - \alpha_i^{f-b}}{2}(e_i - e_{i+1}) = \\ &\quad \frac{\alpha_i^{f+b} + \alpha_i^{f-b}}{2} e_{i-1} + \frac{\alpha_i^{f+b} - \alpha_i^{f-b}}{2} e_{i+1} \\ &\quad -\frac{2\alpha_i^{f+b}}{2} e_i = \frac{\alpha_i^{f-b}}{2}(e_{i-1} - e_{i+1}) \\ &\quad +\frac{\alpha_i^{f+b}}{2} e_{i-1} + \frac{\alpha_i^{f+b}}{2} e_{i+1} - \frac{2\alpha_i^{f+b}}{2} e_i = \\ &\quad \frac{\alpha_i^{f-b}}{2}(e_{i-1} - e_{i+1}) + \frac{\alpha_i^{f+b}}{2}(e_{i-1} + e_{i+1} - 2e_i) = \\ &\quad \frac{\alpha_i^{f-b}}{2N}\frac{(e_{i-1} - e_{i+1})}{1/N} + \frac{\alpha_i^{f+b}}{2N^2}\frac{(e_{i-1} + e_{i+1} - 2e_i)}{1/N^2} \end{aligned} \tag{12}$$

By employing the finite difference approximation, one can write

$$\begin{aligned} \frac{(e_{i-1} - e_{i+1})}{2(1/N)} &= \frac{\partial e(p,t)}{\partial p}|_{p=(N-i)/N} \\ \frac{(\dot{e}_{i-1} - \dot{e}_{i+1})}{2(1/N)} &= \frac{\partial^2 e(p,t)}{\partial p\,\partial t}|_{p=(N-i)/N} \\ \frac{(e_{i-1} - 2e_i + e_{i+1})}{1/N^2} &= \frac{\partial^2 e(p,t)}{\partial p^2}|_{p=(N-i)/N} \\ \frac{(\dot{e}_{i-1} - 2\dot{e}_i + \dot{e}_{i+1})}{1/N^2} &= \frac{\partial^3 e(p,t)}{\partial p^2\,\partial t}|_{p=(N-i)/N} \end{aligned} \tag{13}$$

Therefore, the dynamical equation (10) can be represented by the following partial differential equation.

$$\frac{\partial^2 e}{\partial t^2}+\gamma_i\frac{\partial e}{\partial t}=\frac{\alpha_i^{f-b}}{N}\frac{\partial e}{\partial p} +\frac{\alpha_i^{f+b}}{2N^2}\frac{\partial^2 e}{\partial p^2}+\frac{\gamma_i^{f-b}}{N}\frac{\partial^2 e}{\partial p\partial t}+\frac{\gamma_i^{f+b}}{2N^2}\frac{\partial^3 e}{\partial p^2\partial t} \tag{14}$$

The boundary conditions of (14) depend on the position of the leader in the new coordinate. $p=1$ and $p=0$ are associated with the leader and the last AV in the convoy, respectively. Therefore, one can write

$$e(1,t)=0,\quad \frac{\partial e}{\partial p}(0,t)=0 \tag{15}$$

To achieve the internal stability, the sufficient conditions on control gains should be presented. The following theorem introduces a necessary and sufficient condition on control parameters guaranteeing the zero-tracking error of centralized bi-directional LAVCs.

Theorem 1. Under the following condition, a centralized bi-directional vehicular convoy is internal stable.

$$\gamma_i^b>0 \tag{16}$$

Proof. Since (14) is a linear PDE and according to the boundary conditions (15), the separation of variables method is utilized to solve (14). By replacing $e_i=\sum\chi_m(p)f_m(t)$ in (14), one can write

$$\chi_m\left(\frac{d^2 f_m}{dt^2}+\gamma_i\frac{df_m}{dt}\right)= \frac{f_m}{N^2}\left(\alpha_i^{f-b}N\frac{d\chi_m}{dp}+0.5\alpha_i^{f+b}\frac{d^2\chi_m}{dp^2}\right) +\frac{1}{N^2}\frac{df_m}{dt}\left(\gamma_i^{f-b}N\frac{d\chi_m}{dp}+0.5\gamma_i^{f+b}\frac{d^2\chi_m}{dp^2}\right) \tag{17}$$

If the following conditions hold, the right-hand side of (17) will be presented as a product of two one-variable functions.

$$\frac{\alpha_i^{f-b}}{\alpha_i^{f+b}}=\frac{\gamma_i^{f-b}}{\gamma_i^{f+b}}=\xi_i \tag{18}$$

By replacing (18) in (17), one can write

$$\chi_m\left(\frac{d^2 f_m}{dt^2}+\gamma_i\frac{df_m}{dt}\right)= \frac{0.5}{N^2}\left(2\xi_i N\frac{d\chi_m}{dp}+\frac{d^2\chi_m}{dp^2}\right)\left(\alpha_i^{f+b}f_m+\gamma_i^{f+b}\frac{df_m}{dt}\right) \tag{19}$$

Since the forward control gains α_i^f and γ_i^f are more important than the backward control gains α_i^b and γ_i^b, we define that $\alpha_i^f=\alpha_i^b+\delta_i^\alpha,\gamma_i^f=\gamma_i^b+\delta_i^\gamma$ where δ_i^α and δ_i^γ are the deviation between the position and velocity control gains. Accordingly, one can write

$$\begin{aligned}\alpha_i^{f+b}&=\alpha_i^f+\alpha_i^b=\alpha_i^b+\delta_i^\alpha+\alpha_i^b=\delta_i^\alpha+2\alpha_i^b\\ \alpha_i^{f-b}&=\alpha_i^f-\alpha_i^b=\alpha_i^b+\delta_i^\alpha-\alpha_i^b=\delta_i^\alpha\end{aligned} \tag{20}$$

$$\begin{aligned}\gamma_i^{f+b}&=\gamma_i^f+\gamma_i^b=\gamma_i^b+\delta_i^\gamma+\gamma_i^b=2\gamma_i^b+\delta_i^\gamma\\ \gamma_i^{f-b}&=\gamma_i^f-\gamma_i^b=\gamma_i^b+\delta_i^\gamma-\gamma_i^b=\delta_i^\gamma\end{aligned} \tag{21}$$

Therefore, the constraint can be represented as follows

$$\begin{aligned}&\frac{\alpha_i^{f-b}}{\alpha_i^{f+b}}=\frac{\gamma_i^{f-b}}{\gamma_i^{f+b}}\Rightarrow\frac{\delta_i^\alpha}{\delta_i^\alpha+2\alpha_i^b}=\frac{\delta_i^\gamma}{2\gamma_i^b+\delta_i^\gamma}\Rightarrow\\ &(\delta_i^\alpha+2\alpha_i^b)\delta_i^\gamma=(2\gamma_i^b+\delta_i^\gamma)\delta_i^\alpha\Rightarrow\alpha_i^b\delta_i^\gamma=\gamma_i^b\delta_i^\alpha\\ &\Rightarrow\frac{\alpha_i^b}{\gamma_i^b}=\frac{\delta_i^\alpha}{\delta_i^\gamma}\end{aligned} \tag{22}$$

Equation (19) can be expressed as follows

$$\frac{\chi_m\dfrac{d^2 f_m}{dt^2}}{\alpha_i^{f+b}f_m+\gamma_i^{f+b}\dfrac{df_m}{dt}}= \frac{0.5}{N^2}\left(2\xi_i N\frac{d\chi_m}{dp}+\frac{d^2\chi_m}{dp^2}\right)=-\lambda_m \tag{23}$$

where λ_m is a positive value. From the above equation, we will solve the following ODE in the p domain.

$$\frac{d^2 f_m}{dt^2}+\lambda_m\left(\alpha_i^{f+b}f_m+\gamma_i^{f+b}\frac{df_m}{dt}\right)=0 \tag{24}$$

where λ_m can be calculated from the following boundary value problem

$$\frac{d^2\chi_m}{dp^2}+2\xi_i N\frac{d\chi_m}{dp}-2N^2\lambda_m\chi_m=0 \tag{25}$$

with the following initial conditions

$$\begin{aligned}&\chi_m(1)=0,\\&\frac{d\chi_m}{dp}(0)=0\end{aligned} \tag{26}$$

The solution of ODE (25) is as follows

$$\begin{aligned}\chi_m(p)=e^{-\xi Np}\Big(&c_1\cos\left(N\sqrt{2\lambda_m-\xi^2}\,p\right)+\\&c_2\sin\left(N\sqrt{2\lambda_m-\xi^2}\,p\right)\Big)\end{aligned} \tag{27}$$

By employing the initial conditions (26), one can obtain

$$\begin{aligned}\xi_m(1)=e^{-\xi N}\Big(&c_1\cos\left(N\sqrt{2\lambda_m-\xi^2}\right)+\\&c_2\sin\left(N\sqrt{2\lambda_m-\xi^2}\right)=0\end{aligned}$$

$$\Rightarrow c_1\cos\left(N\sqrt{2\lambda_m-\xi^2}\right)+c_2\sin\left(N\sqrt{2\lambda_m-\xi^2}\right)=0 \tag{28}$$

and

$$\begin{aligned}&\frac{d\chi_m}{dx}(0)=-\xi Nc_1+c_2N\sqrt{2\lambda_m-\xi^2}=0\\&\Rightarrow\frac{c_1}{c_2}=\frac{\sqrt{2\lambda_m-\xi^2}}{\xi}\end{aligned} \tag{29}$$

Combining (28) and (29) will result to

$$\begin{aligned}&\tan\left(N\sqrt{2\lambda_m-\xi^2}\right)=\\&-\frac{\sqrt{2\lambda_m-\xi^2}}{\xi}=-\frac{N\sqrt{2\lambda_m-\xi^2}}{\xi N}\end{aligned} \tag{30}$$

By defining that $\omega_n=N\sqrt{2\lambda_m-\xi^2}$, we will have

$$\begin{aligned}&\tan(\omega_n)=-\frac{\omega_n}{\xi N}=-\frac{\sqrt{2\lambda_m-\xi^2}}{\xi}\\&\Rightarrow\lambda_m=0.5\left(\xi^2+\frac{\omega_m^2}{N^2}\right)\end{aligned} \tag{31}$$

Taking Laplace transform of (24) will result to

$$s_m^2+\left(\lambda_m\gamma_i^{f+b}+\gamma_i\right)s_m+\lambda_m\alpha_i^{f+b}=0 \tag{32}$$

By employing the Routh method, we conclude that if the following inequality holds, (32) is Hurwitz.

$$\eta_i+\lambda_m\left(\gamma_i^f+\gamma_i^b\right)>0 \tag{33}$$

Since $\gamma_i^f>\gamma_i^b$, if $\gamma_i^b>0$ then (33) is assured and the proof is complete.

2.3. Decentralized control design

For decentralized networks, the following control protocol is considered

$$\begin{aligned}u_i=&-\alpha_i^f(e_i-e_{i-1}+D_{i-1,i}+L_{i-1})-\gamma_i^f(\dot e_i-\dot e_{i-1})\\&-\alpha_i^b(e_i-e_{i+1}-D_{i,i+1}-L_i)-\gamma_i^b(\dot e_i-\dot e_{i+1})\end{aligned} \tag{34}$$

The dynamical error of *i*-th AV can be expressed according to

$$\begin{aligned}\ddot e_i=&-\alpha_i^f(e_i-e_{i-1})-\alpha_i^b(e_i-e_{i+1})\\&-\gamma_i^f(\dot e_i-\dot e_{i-1})-\gamma_i^b(\dot e_i-\dot e_{i+1})\end{aligned} \tag{35}$$

Similar to the previous section, the PDE approximation of the above dynamics can be expressed as follows

$$\begin{aligned}\frac{\partial^2 e}{\partial t^2}=&\frac{\alpha_i^{f-b}}{N}\frac{\partial e}{\partial p}+\frac{\alpha_i^{f+b}}{2N^2}\frac{\partial^2 e}{\partial p^2}\\&+\frac{\gamma_i^{f-b}}{N}\frac{\partial^2 e}{\partial p\partial t}+\frac{\gamma_i^{f+b}}{2N^2}\frac{\partial^3 e}{\partial p^2\partial t}\end{aligned} \tag{36}$$

Theorem 2. A decentralized bi-directional LAVC with the consensus protocol (34) is internal stable under the following condition.

$$\gamma_i^b>0 \tag{37}$$

Proof. Similar to theorem 1.

Remark 1. According to theorems 1 and 2, large-scale VCs either centralized and decentralized are internal stable under the same condition. In other words, by employing the PDE approximation to decouple the closed-loop dynamics, we are able to simplify the stability conditions dramatically.

3. String stability of LAVC

The sufficient conditions on control gains satisfying string stability of both centralized and decentralized LAVCs are derived in this section.

3.1. Centralized network

The dynamics of the closed-loop the *i*-th AV under the centralized control (2) is as follows

$$\begin{aligned}\dot{a}_i &= -\alpha_i^f(\dot{x}_i-\dot{x}_{i-1})-\alpha_i^b(\dot{x}_i-\dot{x}_{i+1})\\ &\quad -\gamma_i^f(\ddot{x}_i-\ddot{x}_{i-1})-\gamma_i^b(\ddot{x}_i-\ddot{x}_{i+1})-\eta_i\ddot{x}_i\end{aligned} \tag{38}$$

By taking Laplace transform of (38), one can write

$$\begin{aligned}&\left(s^2+(\gamma_i^f+\gamma_i^b+\eta_i)s+(\alpha_i^f+\alpha_i^b)\right)V_i =\\ &\qquad \left(\alpha_i^f+s\gamma_i^f\right)V_{i-1}+\left(\alpha_i^b+s\gamma_i^b\right)V_{i+1}\end{aligned} \tag{39}$$

This equation can be expressed as follows

$$V_i = G_{i-1}V_{i-1}+G_{i+1}V_{i+1} \tag{40}$$

where

$$G_{i-1}=\frac{\alpha_i^f+s\gamma_i^f}{s^2+(\gamma_i^f+\gamma_i^b+\eta_i)s+(\alpha_i^f+\alpha_i^b)},$$

$$G_{i+1}=\frac{\alpha_i^b+s\gamma_i^b}{s^2+(\gamma_i^f+\gamma_i^b+\eta_i)s+(\alpha_i^f+\alpha_i^b)}.$$

The above relation can be written as follows

$$\begin{aligned}&\frac{V_i}{V_{i-1}}=G_{i-1}+G_{i+1}\frac{V_{i+1}}{V_{i-1}}=G_{i-1}+G_{i+1}\frac{V_{i+1}}{V_i}\frac{V_i}{V_{i-1}}\\ &\frac{V_i}{V_{i-1}}\left(1-G_{i+1}\frac{V_{i+1}}{V_i}\right)=G_{i-1}\Rightarrow\frac{V_i}{V_{i-1}}=\frac{G_{i-1}}{1-G_{i+1}\frac{V_{i+1}}{V_i}}\end{aligned} \tag{41}$$

A convoy of AVs is string stable if and only if [26]

$$\left|\frac{V_i(j\omega)}{V_{i-1}(j\omega)}\right|<1, \qquad \forall\omega>0 \tag{42}$$

Therefore, if $\|G_{i-1}\|_\infty < \|1-G_{i+1}V_{i+1}/V_i\|_\infty$, the convoy is string stable. For the last AV we have $V_N/V_{N-1}=G_{i-1}$. Therefore, if the following inequalities hold, $|V_N/V_{N-1}|<1$ and the convoy is string stable

$$\begin{aligned}&\|G_{i-1}\|_\infty<0.5,\\ &\|G_{i+1}\|_\infty<0.5\end{aligned} \tag{43}$$

Theorem 3. If the condition (44) holds, the LAVC is string stable.

$$\alpha_i^b > \delta_i^\alpha/\sqrt{2} \tag{44}$$

Proof. At first, we analyze the inequality $\|G_{i-1}\|_\infty<0.5$. Consider that $|G_{i-1}(j\omega)|=\sqrt{a_-/b_-}$ where

$$\begin{aligned}a_- &= (\alpha_i^f)^2+\omega^2(\gamma_i^f)^2\\ b_- &= (\alpha_i^f)^2+(\alpha_i^b)^2+2\alpha_i^f\alpha_i^b+\\ &\quad\left(\eta_i^2+2\eta_i(\gamma_i^f+\gamma_i^b)+(\gamma_i^f)^2+\right.\\ &\quad\left.(\gamma_i^b)^2+2\gamma_i^f\gamma_i^b-2\alpha_i^f-2\alpha_i^b\right)\omega^2+\omega^4\end{aligned} \tag{45}$$

If the following inequality satisfies, then $\|G_{i-1}\|_\infty<0.5$

$$\begin{aligned}&(\alpha_i^b)^2-(\alpha_i^f)^2+2\alpha_i^f\alpha_i^b+\\ &\left(\eta_i^2+2\eta_i(\gamma_i^f+\gamma_i^b)+(\gamma_i^b)^2-\right.\\ &\left.(\gamma_i^f)^2+2\gamma_i^f\gamma_i^b-2\alpha_i^f-2\alpha_i^b\right)\omega^2+\omega^4>0\end{aligned} \tag{46}$$

It is a well-known fact that most of the energy of distance errors is at low frequency regions [17]. Therefore, if the coefficient of ω^0 be positive, the string stability is achieved or equivalently $(\alpha_i^b)^2-(\alpha_i^f)^2+2\alpha_i^f\alpha_i^b>0$. By using $\alpha_i^f=\alpha_i^b+\delta_i^\alpha$, we reach to (44). By performing the same procedure for $\|G_{i+1}\|_\infty<0.5$, one can write

$$\begin{aligned}&(\alpha_i^f)^2-(\alpha_i^b)^2+2\alpha_i^f\alpha_i^b+\\ &\left(\eta_i^2+2\eta_i(\gamma_i^f+\gamma_i^b)+(\gamma_i^b)^2-\right.\\ &\left.(\gamma_i^f)^2+2\gamma_i^f\gamma_i^b-2\alpha_i^f-2\alpha_i^b\right)\omega^2+\omega^4>0\end{aligned} \tag{47}$$

Since $\alpha_i^f>\alpha_i^b$, (47) is assured in the low frequency region and the proof is complete.

3.2. Decentralized network

The dynamics of the closed-loop the *i*-th AV under the decentralized control (34) is as follows

$$\begin{aligned}\dot{a}_i &= -\alpha_i^f(\dot{x}_i - \dot{x}_{i-1}) - \alpha_i^b(\dot{x}_i - \dot{x}_{i+1}) \\ &\quad -\gamma_i^f(\ddot{x}_i - \ddot{x}_{i-1}) - \gamma_i^b(\ddot{x}_i - \ddot{x}_{i+1})\end{aligned} \tag{48}$$

By taking Laplace transform of the above equation, we will reach to (40) where

$$\begin{aligned}G_{i-1} &= \frac{\alpha_i^f + s\gamma_i^f}{s^2 + (\gamma_i^f + \gamma_i^b)s + (\alpha_i^f + \alpha_i^b)}, \\ G_{i+1} &= \frac{\alpha_i^b + s\gamma_i^b}{s^2 + (\gamma_i^f + \gamma_i^b)s + (\alpha_i^f + \alpha_i^b)}\end{aligned} \tag{49}$$

Theorem 4. Under the following condition, a decentralized bi-directional vehicular convoy is string stable.

$$\alpha_i^b > \delta_i^\alpha / \sqrt{2} \tag{50}$$

Proof. Similar to theorem 3.

4. Verification studies

In this section, numerical as well as experimental results are provided to illustrate the advantages of the proposed methods in this paper.

4.1. Numerical simulation

In this subsection, a convoy of 10 followers and a leader is considered. In the simulation study, the following constants are investigated: $L_i = 4,\ D_{i,i-1} = 6m, \alpha_i^f = 3.63, \delta_i^\alpha = 1.4,\ \gamma_i^f = 1.17$ and $\delta_i^\gamma = 0.42,\ i = 1,2,...,N$. Moreover, the acceleration profile of the leader is considered as follows with the initial velocity $20m/s$

$$a_0(t) = \begin{cases} 0, & t \le 30\text{s} \\ 1m/s^2, & 30 < t \le 50 \\ 0, & t > 50 \end{cases}.$$

The main objective in vehicular convoying is to move with a constant velocity. Therefore, the accelerating maneuvers of the leader will be considered as an external disturbance. Fig. 4 illustrates the distance error of the centralized convoy. As depicted, the maximum value of distance errors has a decreasing trend by increasing the number of following AVs and the convoy is string stable. On the other hand, all distance errors vanish asymptotically, demonstrating the internal stability. During the accelerating motion of the leader, the distance errors will not vanish but have a decreasing trend along the convoy. In Fig. 5, the velocity of all AVs is depicted. Due to internal stability of LAVC, all following AVs track the leader velocity asymptotically.

Fig. 6 depicts the distance error for the decentralized network. Similarly, the maximum value of distance errors reduces and vanishes asymptotically. So that, the decentralized network is internal as well as string stable. According to Fig. 7, all following AVs' velocity converges to the leader velocity.

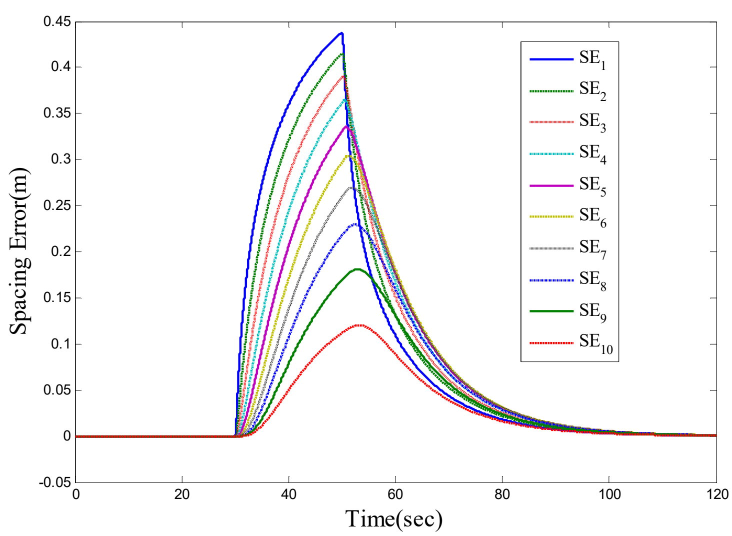

Figure 4: Distance error of the centralized convoy.

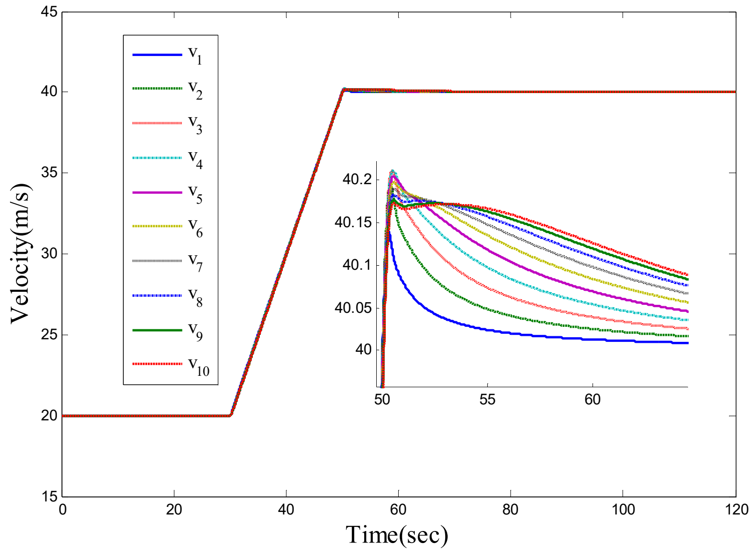

Figure 5: AVs' velocity in centralized convoy.

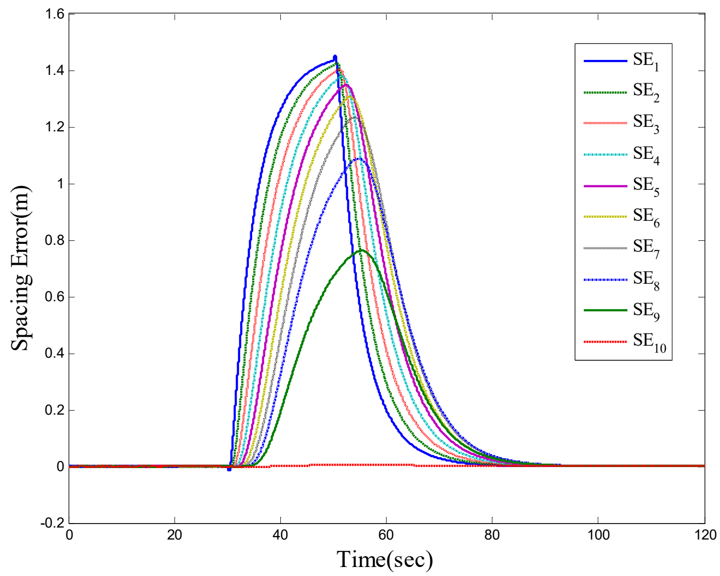

Figure 6: Distance error of the decentralized convoy.

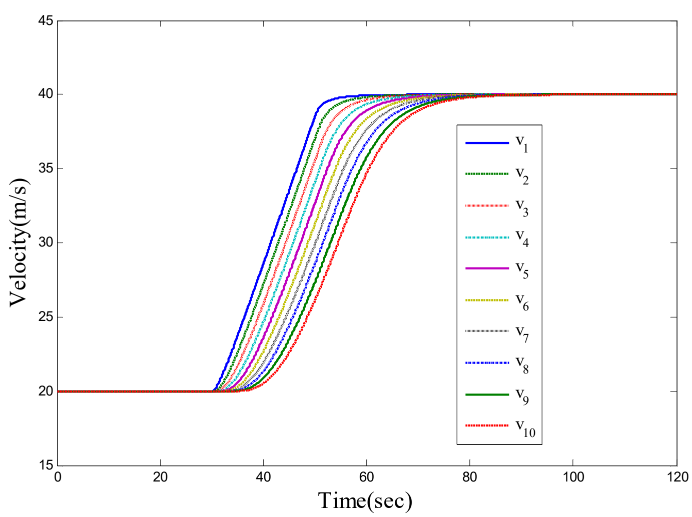

Figure 7: Velocity of AVs in decentralized convoy

4.2. Experimental study

Three four-wheel mobile robots are used to verify the proposed control design methods for practical use. A mobile robot is shown in Fig. 8, which has three infrared distance sensor 2Y0A21 to measure the relative distance of two consecutive robots (the average is used for feedback control). The mobile car is driven by a 12 Volt-140 RPM Buhler DC gear motor and steered by four wheels (10 cm diameter wheel). The longitudinal speed is measured by an encoder on the shaft of the backward wheels. An Arduino Mega 2560 processor onboard for each mobile robot functions as the real-time computing and control unit.

In the experimental study, the leader has the constant velocity 20cm/s during [0,5]s. After that, the velocity increases from 20cm/s to 28 cm/s during [5, 10]s, and keeps constant velocity 28 cm/s again during [10, 15]s. The desired inter-AV distance is assumed to be 25cm. Moreover, due to low velocity of mobile cars, the air drag force is not considered.

Table 1 presents the characteristics of mobile robots employed in the experimental studies.

Figs. 9 and 10 depict the distance error and velocity of leading and following mobile robots, respectively. According to these figures, both internal and string stability of convoy are achieved.

Table 1. Charactristics of the mobile robots

Type of distance sensor	Infrared 2Y0A21
Type of DC motor	12 Volt-140 RPM Buhler
Diameter of front wheels	10 cm
Diameter of rear wheels	10 cm
Type of processor	Arduino Mega 2560
Initial leader velocity	20 cm/s
Safe distancing	25 cm

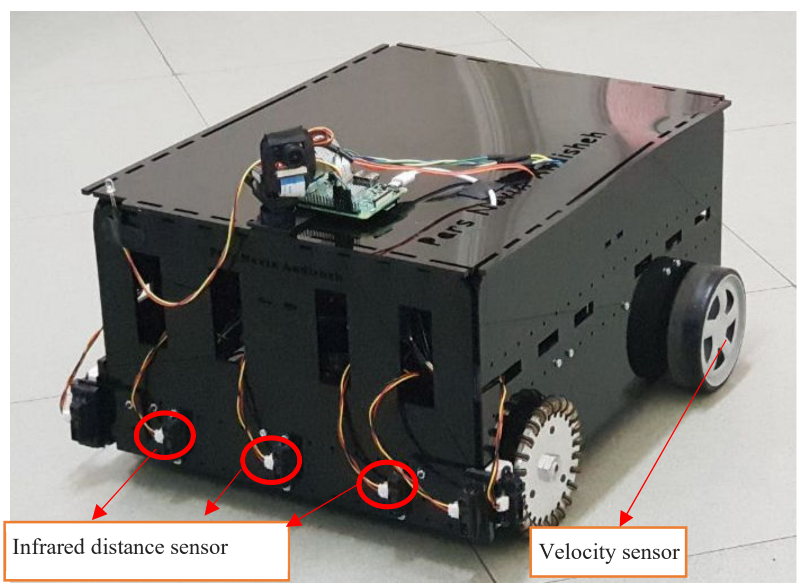

Figure 8: The following mobile robot.

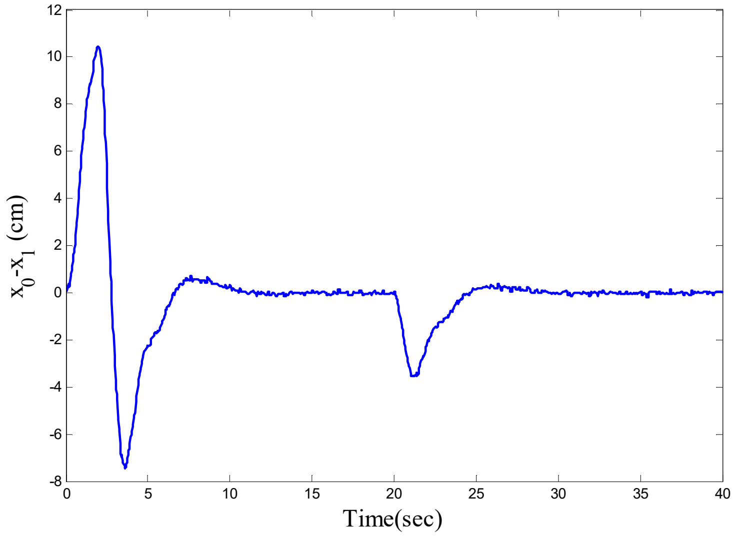

Figure 9: Distance tracking error of robot convoy.

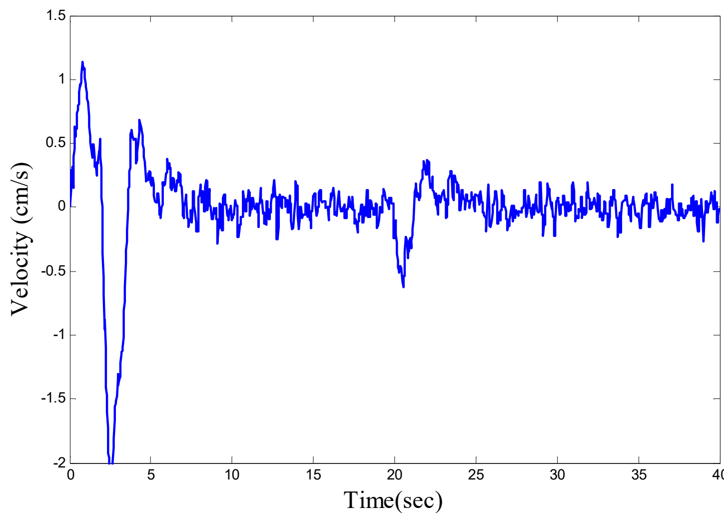

Figure 10: Velocity tracking error of robot convoy.

4.3. Brief discussion and comparisons

Figs. 4 and 9 illustrate the efficiency of the proposed method in theorems 1-4. Both centralized and decentralized methods presented in section 3 guarantee the internal and string stability of LAVCs without any limitations. In other words, the conditions (16), (37), (44) and (50) are satisfied easily and therefore, the internal and string stability of the closed-loop dynamics are assured. In other words, compared with most of the previous studies, the presented method introduces more simple conditions on control parameters.

5. Conclusion

The problems of internal (asymptotic) as well as string stability of centralized and decentralized LAVCs with bi-directional communication topology were investigated in this paper. A linear control utilizing the relative displacement and velocity compared with forward and backward AVs was designed. By introducing a PDE-based approach, the dynamics of the closed-loop system was decoupled and simplified. For each decoupled dynamical system, the necessary inequalities satisfying internal stability as well as string stability were introduced. Simulation and experimental results were provided to describe the merits of this algorithm.

Research funding information

The author declares the reception of the following financial support for the research, authorship, and/or publication of this paper. The author thankfully appreciates the University of Ayatollah Boroujerdi for providing the financial support with the grant number 15664-214255.

List of symbols

x : Position of each AV

v : Velocity of each AV

a: Acceleration of each AV

u: Control input of each AV

α^f : Forward position gain

α^b : Backward position gain

γ^f : Forward velocity gain

γ^b : Backward velocity gain

D: Safe inter-vehicle spacing

L: Length of each AV

η : A positive gain

N: Number of AVs

e: Position error

G: Transfer function

V: Laplace transform of velocity

$x_{i,d}$ Desired position of the *i*-th vehicle

E Error vector

t Time

ω : Frequency

References

[1] H. Ge, R. Cheng, and L. Lei, "The theoretical analysis of the lattice hydrodynamic models for traffic flow theory," *Physica A: Statistical Mechanics and its Applications,* vol. 389, pp. 2825-2834, 2010.

[2] N. Wan, A. Vahidi, and A. Luckow, "Optimal speed advisory for connected vehicles in arterial roads and the impact on mixed traffic," *Transportation Research Part C: Emerging Technologies,* vol. 69, pp. 548-563, 2016.

[3] J. Zhang, T. Feng, F. Yan, S. Qiao, and X. Wang, "Analysis and design on intervehicle distance control of autonomous vehicle platoons," *ISA Transactions,* vol. 100, pp. 446-453, 2020.

[4] G. J. Naus, R. P. Vugts, J. Ploeg, M. J. van De Molengraft, and M. Steinbuch, "String-stable CACC design and experimental validation: A frequency-domain approach," *IEEE Transactions on vehicular technology,* vol. 59, pp. 4268-4279, 2010.

[5] C. Wang and H. Nijmeijer, "String stable heterogeneous vehicle platoon using cooperative adaptive cruise control," in *2015 IEEE 18th International Conference on Intelligent Transportation Systems*, 2015, pp. 1977-1982.

[6] H. Chehardoli, A. Ghasemi, and A. Najafi, "Centralized and decentralized distributed control of longitudinal vehicular platoons with non-uniform communication topology," *Asian Journal of Control,* vol. 21, pp. 2691-2699, 2019.

[7] A. Petrillo, A. Salvi, S. Santini, and A. S. Valente, "Adaptive multi-agents synchronization for collaborative driving of autonomous vehicles with multiple communication delays," *Transportation research part C: emerging technologies,* vol. 86, pp. 372-392, 2018.

[8] L. Zhang and G. Orosz, "Motif-based design for connected vehicle systems in presence of heterogeneous connectivity structures and time delays," *IEEE*

Transactions on Intelligent Transportation Systems, vol. 17, pp. 1638-1651, 2016.

[9] P. Wijnbergen and B. Besselink, "Existence of decentralized controllers for vehicle platoons: On the role of spacing policies and available measurements," *Systems & Control Letters,* vol. 145, pp. 1-9, 2020.

[10] Y. Bian, Y. Zheng, W. Ren, S. E. Li, J. Wang, and K. Li, "Reducing time headway for platooning of connected vehicles via V2V communication," *Transportation Research Part C: Emerging Technologies,* vol. 102, pp. 87-105, 2019.

[11] P. A. Cook, "Stable control of vehicle convoys for safety and comfort," *IEEE transactions on automatic control,* vol. 52, pp. 526-531, 2007.

[12] H. Wei, Q. Sun, J. Chen, and Y. Shi, "Robust distributed model predictive platooning control for heterogeneous autonomous surface vehicles," *Control Engineering Practice,* vol. 107, pp. 1-8, 2021.

[13] B. Samani and A. H. Shamekhi, "Design of real-time cruise controller with trained neural network using multi-objective predictive adaptive controller data to reducing fuel consumption and increasing comfort," *Automotive Science and Engineering,* vol. 11, pp. 3472-3484, 2021.

[14] Y. Zheng, S. E. Li, J. Wang, D. Cao, and K. Li, "Stability and scalability of homogeneous vehicular platoon: Study on the influence of information flow topologies," *IEEE Transactions on intelligent transportation systems,* vol. 17, pp. 14-26, 2015.

[15] X. Guo, J. Wang, F. Liao, and R. S. H. Teo, "Distributed adaptive integrated-sliding-mode controller synthesis for string stability of vehicle platoons," *IEEE Transactions on Intelligent Transportation Systems,* vol. 17, pp. 2419-2429, 2016.

[16] L. Xu, W. Zhuang, G. Yin, and C. Bian, "Energy-oriented cruising strategy design of vehicle platoon considering communication delay and disturbance," *Transportation Research Part C: Emerging Technologies,* vol. 107, pp. 34-53, 2019/10/01/ 2019.

[17] H. Chehardoli, "Multi look-ahead consensus of vehicular networks in the presence of random data missing," *Journal of Vibration and Control,* pp. 1-11, 2021.

[18] G. Guo and D. Li, "Adaptive Sliding Mode Control of Vehicular Platoons With Prescribed Tracking Performance," *IEEE Transactions on Vehicular Technology,* vol. 68, pp. 7511-7520, 2019.

[19] P. Cook, "Conditions for string stability," *Systems & control letters,* vol. 54, pp. 991-998, 2005.

[20] M. Di Bernardo, A. Salvi, and S. Santini, "Distributed consensus strategy for platooning of vehicles in the presence of time-varying heterogeneous communication delays," *IEEE Transactions on Intelligent Transportation Systems,* vol. 16, pp. 102-112, 2014.

[21] H. Chehardoli, A. Ghasemi, and M. Daneshyian, "An optimal consensus to guarantee the stability and crash avoidance of large-scale traffic flow in presence of time delay," *Automotive Science and Engineering,* vol. 10, pp. 3434-3445, 2020.

[22] S. Santini, A. Salvi, A. S. Valente, A. Pescapé, M. Segata, and R. L. Cigno, "A consensus-based approach for platooning with intervehicular communications and its validation in realistic scenarios," *IEEE Transactions on Vehicular Technology,* vol. 66, pp. 1985-1999, 2016.

[23] F. Gao, S. E. Li, Y. Zheng, and D. Kum, "Robust control of heterogeneous vehicular platoon with uncertain dynamics and communication delay," *IET Intelligent Transport Systems,* vol. 10, pp. 503-513, 2016.

[24] H. Chehardoli and M. R. Homaeinezhad, "Stable control of a heterogeneous platoon of vehicles with switched interaction topology, time-varying communication delay and lag of actuator," *Proceedings of the Institution of Mechanical Engineers, Part C: Journal of Mechanical*

Engineering Science, vol. 231, pp. 4197-4208, 2017.

[25] S. E. Li, X. Qin, Y. Zheng, J. Wang, K. Li, and H. Zhang, "Distributed platoon control under topologies with complex eigenvalues: Stability analysis and controller synthesis," *IEEE Transactions on Control Systems Technology,* vol. 27, pp. 206-220, 2017.

[26] R. Rajamani, *Vehicle dynamics and control*: Springer Science & Business Media, 2011.

[27] H. Chehardoli and M. Homainezhad, "Internal and string stability analyses of longitudinal platoon of vehicles with communication delay and actuator lag under constant spacing policy," *Automotive Science and Engineering,* vol. 7, pp. 2482-2494, 2017.